Structural and Spectroscopic Studies of the Versatile Coordination Chemistry of the Chiral Ligand *N*,*N*-Bis(1-propan-2-onyl oxime)-L-methionine *N*′-Methylamide with Ni^{II} and Zn^{II}

Dell T. Rosa, Jeanette A. Krause Bauer, and Michael J. Baldwin*

Department of Chemistry, University of Cincinnati, P.O. Box 210172, Cincinnati, Ohio 45221-0172

Received August 22, 2000

The potentially pentadentate, chiral ligand *N*,*N*-bis(1-propan-2-onyl oxime)-L-methionine *N*′-methylamide (L-MABO) shows remarkable versatility in its coordination chemistry with Ni(II) and Zn(II). In the crystal structure of the $ZnCl_2$ complex of L-MABO, the ligand coordinates to the metal only through its three nitrogen donor groups (one amine and two oximes), with two chloride anions completing the distorted trigonal bipyramidal coordination sphere. In the $NiCl_2$ complex, the three nitrogen donors and the thioether sulfur coordinate, along with two chlorides. The crystal structure of the $Ni(NO_3)_2$ complex contains two independent molecules, one of which coordinates the three nitrogens, the thioether sulfur, and the amide oxygen of L-MABO in addition to one nitrate anion. The second molecule coordinates the three nitrogen donors, the amide oxygen, one nitrate anion, and a methanol molecule. Thus, in only three crystal structures, L-MABO demonstrates its ability to provide N_3, N_3S, N_3O, and N_3OS donor sets. The thioether-bound complexes are unusual in that they have a predominantly nitrogen environment with a nickel−thioether bond that is not constrained by surrounding donor groups in a macrocyclic or linear polydentate motif. Comparison of the thioether-coordinated and methanol-coordinated molecules in the $Ni(NO_3)$ salt of L-MABO demonstrate the effect of the thioether bond on the relative "hardness" of the nickel. The electronic absorption and circular dichroism spectra of the aqueous solutions of the nickel complexes are interpreted in terms of a "descent in symmetry" model based on successive C_{3v} and C_s distortions from octahedral geometry. These ligand field spectra indicate that in aqueous solution all ligand groups except for the three nitrogens of L-MABO are displaced by water. In acetonitrile, the non-nitrogen donors in the nitrate salt may also be displaced, while the chlorides remain coordinated.

Introduction

We have recently designed and synthesized[1] a series of ligands with mixtures of oxime and amide donor groups in a tripodal amine framework that are designed to stabilize the higher oxidation states of nickel, Ni(III) and Ni(IV), and perhaps promote reactions of the Ni(II) complexes with oxygen upon deprotonation of the ligand. Amidates are well-known to stabilize high oxidation state metal complexes, including Ni(III)[2,3] and rarely Ni(IV).[4] Oximates also stabilize higher oxidation states of nickel, often preferring Ni(IV) with respect to disproportionation of Ni(III). [5,6] Additionally, oximes may be considered to be reasonable models for the biologically important imidazole donor group of the amino acid histidine. Like other groups used to model histidine, such as pyridyl or pyrazole, the oxime nitrogen has the same sp^2 hybridization as imidazole. However, unlike pyridyl, or the pyrazole groups in polydentate ligands connected through one of the nitrogens, the oximes may be deprotonated at a position other than the coordinating atom, similar to histidine.

Incorporation of additional biologically relevant donor groups into these ligands is achieved by using natural amino acids as starting materials.[1] This provides a potential fifth donor group as well as a chiral center that allows the use of circular dichroism as an additional spectroscopic tool. In the complexes that are the subject of this paper, L-methionine is used as the starting material resulting in the potentially pentadentate, chiral ligand *N*,*N*-bis(1-propan-2-onyl oxime)-L-methionine *N*′-methylamide (L-MABO, for L-methionine amide bis oxime), with two oximes,

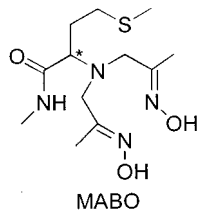

MABO

an amide, a tertiary amine, and a thioether available for coordination. As anticipated on the basis of the ability of oximates to stabilize higher oxidation states of nickel, deprotonation of the oxime groups results in reaction of the Ni(II) complexes of L-MABO with O_2.[7,8] Formation of a stable Ni(III)

* Author to whom correspondence should be addressed. Fax: (513) 556-9239. E-mail: michael.baldwin@uc.edu.

(1) Goldcamp, M. J.; Rosa, D. T.; Landers, N. A.; Mandel, S. M.; Krause Bauer, J. A.; Baldwin, M. J. *Synthesis* **2000**, 2033−2038.
(2) Kimura, E.; Machida, R.; Kodama, M. *J. Am. Chem. Soc.* **1984**, *106*, 5497−5505.
(3) Collins, T. J.; Nichols, T. R.; Uffelman, E. S. *J. Am. Chem. Soc.* **1991**, *113*, 4708−4709.
(4) Patra, A. K.; Mukherjee, R. *Inorg. Chem.* **1999**, *38*, 1388−1393.
(5) Mohanty, J. G.; Singh, R. P.; Chakravorty, A. *Inorg. Chem.* **1975**, *14*, 2178−2183.
(6) Singh, A. N.; Chakravorty, A. *Inorg. Chem.* **1980**, *19*, 969−971.
(7) Rosa, D. T.; Goldcamp, M. J.; Mandel, S.; Krause Bauer, J. A.; Baldwin, M. J. *Abstracts of Papers*, 220th National Meeting of the American Chemical Society, Washington, DC, August 2000; American Chemical Society: Washington, DC, 2000; Abstract 120.
(8) Goldcamp, M. J.; Rosa, D. T.; Landers, N.; Krause-Bauer, J. A.; Baldwin, M. J. *Abstracts of Papers*, 220th National Meeting of the American Chemical Society, Washington, DC, August 2000; American Chemical Society: Washington, DC, 2000; Abstract 118.

10.1021/ic000971f CCC: $20.00
Published on Web 03/01/2001

complex in these reactions has been demonstrated by EPR spectroscopy.[9] To sort out the mechanism of the oxygen reactions of this and related Ni(II) complexes, it is first necessary to determine the structures of the starting complexes prior to deprotonation and oxidation. Here, we describe the structures and spectroscopy of several Ni(II) and Zn(II) complexes of the neutral L-MABO ligand.

In these chiral complexes, L-MABO acts as a tri-, tetra-, or pentadentate ligand providing N_3, N_3S, N_3O, and N_3OS donor sets. Combinations of nitrogen and sulfur donors are common to a number of known nickel metalloenzymes, including the recently discovered Ni-dependent superoxide dismutase,[10] the α subunit of CO dehydrogenase,[11] and 2-mercaptoethanol-inhibited urease.[12] The F_{430} cofactor of methyl-coenzyme M reductase has nickel in an N_4-donating corphin that allows axial coordination.[13] Although a mechanism in which the methyl thioether sulfur of methyl-coenzyme M coordinates to the nickel is considered unlikely, an inactive form of the enzyme has been shown to have the thiol sulfur of coenzyme M coordinated to the nickel,[14] and an intermediate involving coordination of the coenzyme B sulfur has recently been proposed.[15] Often, structural information about the coordination environment of the active site metal in metalloenzymes is determined by EXAFS (extended X-ray absorption fine structure) spectroscopy, and an appropriate variety of structurally characterized model complexes is needed for calibration of this method. The importance of appropriate models has been demonstrated by Penner-Hahn and co-workers[16] in thorough studies of the parameters necessary for accurate interpretation of the EXAFS of Zn metalloenzymes with mixed N/S environments. The Ni(II) structures reported here are unusual in that they provide a mixed N/O and thioether coordination environment with a "branched" polydentate ligand rather than the macrocyclic or "linear" polydentate ligands in which the thioether coordination is constrained by the surrounding donor groups.

The chirality of the complexes permits more detailed exploration of the electronic structure through circular dichroism (CD) spectroscopy. The solution structures of the nickel complexes are addressed by analysis of the ligand field spectra using Gaussian fits of the absorption and CD data. The large differences in the donor ability of the various coordinating groups of the ligand produce energy splittings between the absorption and CD bands within the different ligand field transition manifolds. These data provide an excellent example of the utility of successive descents in symmetry from an idealized octahedral geometry in the interpretation of the ligand field spectra.

Experimental Section

Materials. Acetonitrile was obtained from Fisher Scientific and stirred over anhydrous Cu_2SO_4 to remove any amines, dried over calcium hydride, and distilled from P_2O_5. Water was purified by filtration through a Barnstead/Thermolyne deionizing column and then distilled from a Corning Mega-Pure System MP-3A. *N*,*N*-Bis(1-propan-2-onyl oxime)-L-methionine *N*′-methylamide (L-MABO) was prepared as described previously.[1] All other chemicals were obtained from commercial sources and used without further purification.

Synthesis of Complexes. [Zn(L-MABO)Cl$_2$] (1). A solution of zinc chloride (0.420 g, 3.29 mmol) in 30 mL of methanol was added with stirring to a solution of L-MABO (1.00 g, 3.29 mmol) in 30 mL of methanol. The colorless solution was layered with 150 mL of ethyl acetate and allowed to diffuse. Colorless, needlelike, X-ray quality crystals precipitated within 2 days and were isolated by filtration (yield: 1.14 g, 79%). ^{1}H NMR (DMSO-d_6): 10.55 (s, 2H), 7.61 (b, 1H), 3.15 (m, 1H), 3.11 (m, 4H), 2.59 (d, 3H, J = 4.07 Hz), 2.44 (t, 2H, J = 7.17 Hz), 2.04 (s, 3H), 1.82 (m, 2H), 1.73 (s, 6H). ^{13}C NMR (DMSO-d_6): 172.08, 154.43, 61.72, 54.79, 30.97, 27.44, 25.79, 14.96, 12.48. Anal. Calcd for $ZnC_{12}H_{24}N_4O_3SCl_2$: C, 32.68; H, 5.45; N, 12.71. Found: C, 32.82; H, 5.19; N, 12.84.

[Ni(L-MABO)Cl$_2$] (2). A solution of nickel chloride hexahydrate (0.78 g, 3.29 mmol) in 30 mL of methanol was added with stirring to a solution of L-MABO (1.00 g, 3.29 mmol) in 30 mL of methanol. The blue solution was layered with 150 mL of ethyl acetate and allowed to diffuse. Blue, needlelike, X-ray quality crystals precipitated within a few hours and were isolated the next day by filtration (yield: 1.21 g, 85%). μ_{eff} (297 K): 3.2 μ_B Anal. Calcd for $NiC_{12}H_{24}N_4O_3SCl_2$: C, 33.20; H, 5.53; N, 12.91. Found: C, 33.43; H, 5.33; N, 12.71.

[Ni(L-MABO)(NO$_3$)][NO$_3$]·1.5CH$_3$OH (3). A solution of nickel nitrate hexahydrate (0.96 g, 3.29 mmol) in 30 mL of methanol was added with stirring to a solution of L-MABO (1.00 g, 3.29 mmol) in 30 mL of methanol. The blue solution was layered with 150 mL of ethyl acetate and allowed to diffuse. Blue, needlelike, X-ray quality crystals precipitated within a few hours and were isolated the next day by filtration (yield: 1.21 g, 67%). μ_{eff} (297 K): 3.3 μ_B Anal. Calcd for $NiC_{12}H_{24}N_6O_9S\cdot1.5CH_3OH$: C, 30.30; H, 5.61; N, 15.71. Found: C, 30.62; H, 5.54; N, 15.54.

Physical Measurements. Absorption spectra were obtained on a CARY-14 spectrophotometer with a PC interface supplied by OLIS, Inc. Circular dichroism (CD) spectra were recorded on a Jasco J-715 spectropolarimeter with a PC interface and were baseline corrected by subtraction of a spectrum of solvent in the same 1 cm quartz cell. The absorption and CD spectra were fit with the minimum number of Gaussian functions required for a reasonable simulation of the data using a nonlinear algorithm in the GRAMS/32 software package.

^{1}H and ^{13}C NMR spectra were obtained on a Bruker AC-250 instrument and are reported in ppm vs TMS. Quantitative Technologies, Inc. (Whitehouse, NJ), carried out the elemental analyses. Magnetic moments were measured at room temperature (297 K) using a finely ground powder packed in Alfa Aesar 3.24 mm i.d. quartz sample tubes on a Johnson Matthey magnetic susceptibility balance. Conductivity measurements were made using a Yellow Springs Instrument Co. model 31A conductivity bridge with a model 3401 platinum electrode. Solutions were prepared in the same fashion as those used in the spectroscopic experiments, and measurements were made in triplicate.

Samples for mid-infrared spectra were dispersed in a KBr pellet, and samples for far-infrared spectra were dispersed in a Nujol mull and spread on a CsI pellet. A BioRad Excalibur spectrometer with a DTGS electrically cooled detector with a KBr extended range beam splitter was used for the mid-IR, and the same platform with a DTGS far-IR detector with a Mylar 6.25 μm beam splitter was used for the far-IR. Raman samples were prepared by finely grinding the crystalline material with Na_2SO_4 (10 wt %) and packing it into 1 mm i.d. melting point capillary tubes. Samples were spun at 5000 rpm using a Dremel Moto-Tool during data collection. Raman spectra were obtained using a SPEX 1404 0.85 m double spectrometer with a liquid N_2 cooled, 13.6 mm back-thinned SPEX CCD chip detector. Raman scattering was excited at 488 nm (~300 mW at the sample) with a Coherent 10 W Sabre Ar ion laser and collected from 275 to 2000 cm^{-1} using a Kaiser Optical Systems holographic SuperNotch filter to modulate the Raleigh line. Raman shifts were calibrated against the laser emission at 488.0 nm.

(9) Rosa, D. T.; Baldwin, M. J. Unpublished results.
(10) Choudhury, S. B.; Lee, J.-W.; Davidson, G.; Yim, Y.-I.; Bose, K.; Sharma, M. L.; Kang, S.-O.; Cabelli, D. E.; Maroney, M. J. *Biochemistry* **1999**, *38*, 3744−3752.
(11) Xia, J.; Dong, J.; Wang, S.; Scott, R. A.; Lindahl, P. A. *J. Am. Chem. Soc.* **1995**, *117*, 7065−7070.
(12) Wang, S.; Lee, M. H.; Hausinger, R. P.; Clark, P. A.; Wilcox, D. E.; Scott, R. A. *Inorg. Chem.* **1994**, *33*, 1589−1593.
(13) Hausinger, R. P. *Biochemistry of Nickel*; Plenum Press: New York, 1993.
(14) Ermler, U.; Grabarse, W.; Shima, S.; Goulbeaud, M.; Thauer, R. K. *Science* **1997**, *278*, 1457−1462.
(15) Signor, L.; Knuppe, C.; Hug, R.; Schweizer, B.; Pfaltz, A.; Jaun, B. *Chem.—Eur. J.* **2000**, *6*, 3508−3516.
(16) Clark-Baldwin, K.; Tierney, D. L.; Govindaswamy, N.; Gruff, E. S.; Kim, C.; Berg, J.; Koch, S. A.; Penner-Hahn, J. E. *J. Am. Chem. Soc.* **1998**, *120*, 8401−8409.

Table 1. Crystallographic Data and Structure Refinement for **1**, **2**, and **3**

	1	**2**	**3**
empirical formula	$ZnC_{12}H_{24}N_4O_3SCl_2$	$NiC_{12}H_{24}N_4O_3SCl_2$	$NiC_{12}H_{24}N_5O_6S]NO_3 \cdot [NiC_{13}H_{28}N_5O_7S]NO_3$
fw	440.68	434.02	1022.35
temp (K)	294(2)	150(2)	150(2)
cryst syst	orthorhombic	hexagonal	monoclinic
space group	$P2_12_12_1$	$P6_5$	$P2_1$
unit cell dimens			
a (Å)	8.6833(2)	12.4125(2)	10.1231(2)
b (Å)	10.4612(2)	12.4125(2)	16.5442(6)
c (Å)	21.0386(3)	23.0975(8)	13.6701(5)
α (deg)	90	90	90
β (deg)	90	90	104.446(2)
γ (deg)	90	120	90
vol (Å^3), Z	1911.10(6), 4	3081.87(13), 6	2217.06(12), 2
density (calcd) (Mg/m^3)	1.532	1.403	1.530
abs coeff (mm^{-1})	1.691	1.321	1.026
Flack param	0.01(1)	−0.02(2)	0.02(2)
final R indices [$I > 2\sigma(I)$]			
R1	0.0314	0.0472	0.0553
wR2	0.0676	0.1110	0.1301
R indices (all data)			
R1	0.0402	0.0645	0.0692
wR2	0.0711	0.1203	0.1373

X-ray Crystallography. General Procedures. A suitable crystal was mounted on the tip of a glass fiber for data collection. Data were collected[17] on a Siemens SMART 1K CCD diffractometer (program v5.051, sealed-tube generator, graphite-monochromated Mo Kα radiation). The detector was 5 cm from the crystal. A series of data frames measured at 0.3° increments of ω were collected to calculate a unit cell. Data collection frames were measured at 0.3° intervals of ω. The data frames were processed using the program SAINT v5.A06 (Bruker AXS, Madison, WI). The data were corrected for decay, Lorentz, and polarization effects. Semiempirical absorption correction based on the multiscan technique and beam corrections were applied using SADABS.[18]

Structures were solved by a combination of direct methods using SHELXTL v5.03 and the difference Fourier technique and refined by full-matrix least squares on F^2 for the reflections diffracting out to 0.75 Å.[19] The molecules each contain a chiral center, and the absolute configuration was determined on the basis of refinement of the Flack parameter and the effect on the overall R-factor. Non-hydrogen atoms were refined with anisotropic displacement parameters. Hydrogen atom isotropic temperature factors were defined as $U(C)a = U(H)$ where $a = 1.2$ for NH, CH, or CH_2 hydrogens, and $a = 1.5$ for OH or CH_3 hydrogens. Hydrogen atoms were either located directly or calculated on the basis of geometric criteria (methyl H atoms were calculated after locating at least one directly) and treated with a riding model. Disordered methyl groups appear in all three complexes; occupancies for the H atoms were set at 0.5. A suitable disorder model for the methanol solvate in complex **3** could not be resolved; thus the solvent contribution was subtracted from the reflection data using the program SQUEEZE.[20] The electrons/unit cell from the solvent were applied to the molecular weight, $F(000)$, and density values reported. Elemental analysis suggests at least 1 fully occupied methanol of crystallization. The final difference map in each case was essentially featureless. Crystallographic data are summarized in Table 1. Final atomic coordinates, displacement parameters, bond distances and angles, and H-bonds are provided as Supporting Information.

(17) Data were collected through the Ohio Crystallographic Consortium, funded by the Ohio Board of Regents 1995 Investment Fund (CAP-075) located at the University of Toledo, Instrumentation Center in A&S, Toledo, OH 43606.
(18) Sheldrick, G. M. University of Goettingen, Germany.
(19) G. M. Sheldrick, University of Goettingen, Germany, and Bruker AXS, Madison, WI.
(20) Spek, A. L. 1992, University of Utrecht, Utrecht, The Netherlands. SQUEEZE is a routine implemented in PLATON-92 that allows solvent contributions to be eliminated from the reflection data.

Results

Structure Descriptions. Figure 1 shows the crystal structure of the Zn(II) complex **1**. Selected bond distances and angles are given in Table 2. The molecule crystallizes with only a single zinc complex in the asymmetric unit and no solvent of crystallization. The Zn(II) ion coordinates the ligand L-MABO through its two oxime nitrogens and the tertiary amine. The thioether and amide arms extend out into the lattice. The amide hydrogen participates in a rather weak H-bond with Cl(1) from another molecule (N(1)−H(1)···Cl(1); N(1)···Cl(1), 3.582(3) Å; H(1)···Cl(1), 2.82 Å). The remaining coordination sphere is filled by the two chlorine anions giving a structure best described

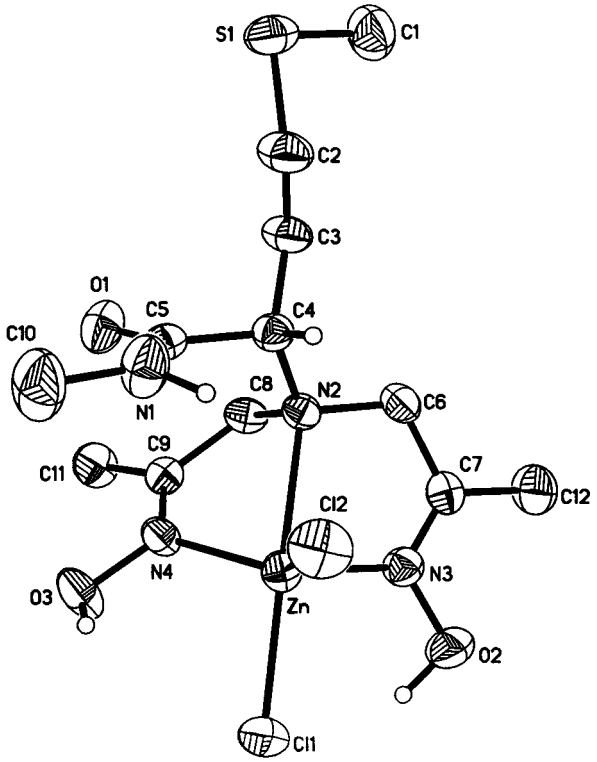

Figure 1. ORTEP view (50% probability) of the neutral complex [Zn(L-MABO)Cl_2] (**1**). Methylene and methyl hydrogen atoms are omitted for clarity.

Table 2. Selected Bond Distances (Å) and Angles (deg) of $ZnC_{12}H_{24}N_4O_3SCl_2$ (**1**) and $NiC_{12}H_{24}N_4O_3SCl_2$ (**2**)

1		**2**	
Zn−N(2)	2.411(2) amine	Ni−N(1)	2.213(3) amine
Zn−N(3)	2.078(2)	Ni−N(2)	2.028(3)
Zn−N(4)	2.056(2)	Ni−N(3)	2.014(3)
		Ni−S	2.3676(11)
Zn−Cl(1)	2.3474(7)	Ni−Cl(1)	2.3532(11)
Zn−Cl(2)	2.2325(7)	Ni−Cl(2)	2.4572(11)
N(2)−Zn−N(3)	73.65(7)	N(1)−Ni−N(2)	79.61(13)
N(3)−Zn−N(4)	115.85(8)	N(2)−Ni−N(3)	90.52(14)
N(4)−Zn−N(2)	73.83(7)	N(3)−Ni−N(1)	79.35(13)
N(2)−Zn−Cl(1)	154.75(5)	N(1)−Ni−Cl(1)	96.78(9)
N(3)−Zn−Cl(1)	92.28(6)	N(2)−Ni−Cl(1)	176.34(10)
N(4)−Zn−Cl(1)	94.74(6)	N(3)−Ni−Cl(1)	89.35(10)
N(2)−Zn−Cl(2)	97.75(5)	N(1)−Ni−Cl(2)	162.58(9)
N(3)−Zn−Cl(2)	109.16(6)	N(2)−Ni−Cl(2)	87.31(10)
N(4)−Zn−Cl(2)	128.86(7)	N(3)−Ni−Cl(2)	89.40(10)
		N(1)−Ni−S	99.97(9)
		N(2)−Ni−S	94.59(10)
		N(3)−Ni−S	174.64(10)
		Cl(1)−Ni−S	85.45(4)
		Cl(2)−Ni−S	92.45(4)

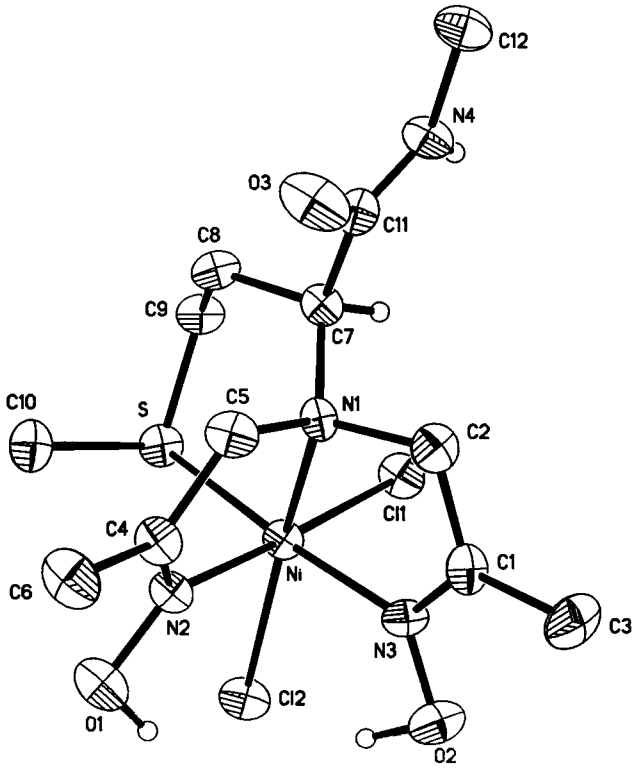

Figure 2. ORTEP view (50% probability) of the neutral complex [Ni(L-MABO)Cl_2] (**2**). Methylene and methyl hydrogen atoms are omitted for clarity.

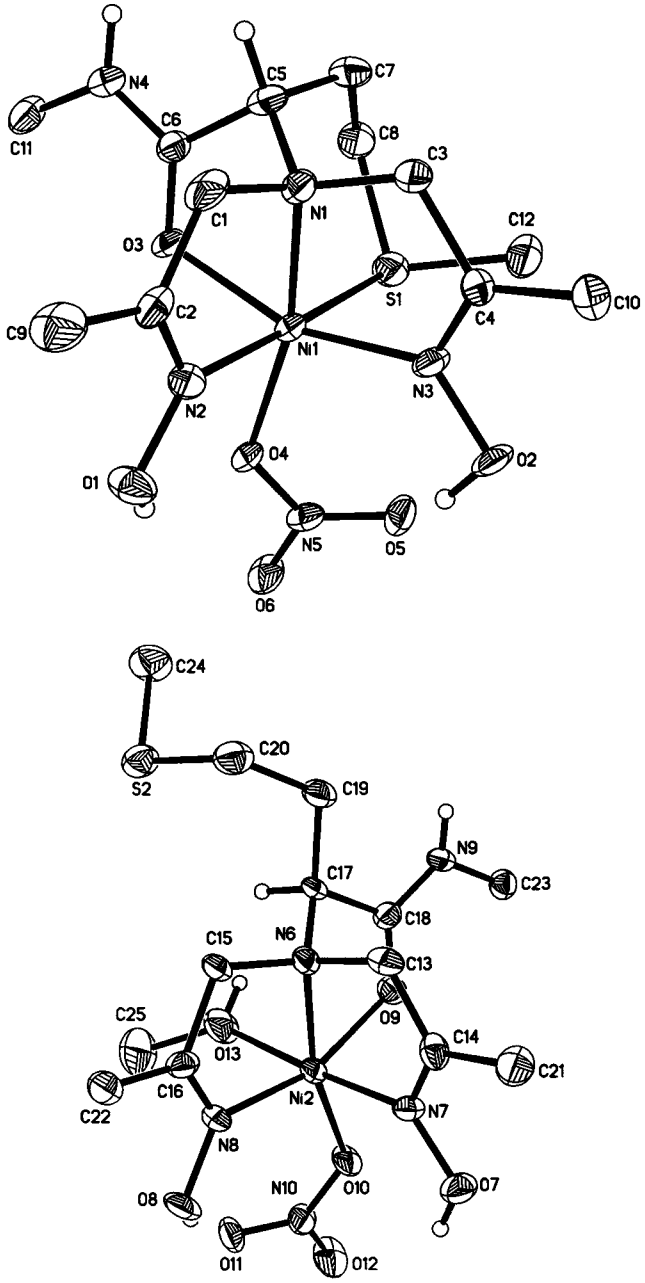

Figure 3. ORTEP views (50% probability) of the complex cations [Ni(L-MABO)(NO_3)][NO_3] (**3a**) and [Ni(L-MABO)$(NO_3)(CH_3OH)$]-[NO_3] (**3b**). Methylene and methyl hydrogen atoms are omitted for clarity.

as distorted trigonal bipyramidal with N(4), N(3), and Cl(2) defining the equatorial plane, and N(2) and Cl(1) as axial ligands. The axial chloride [Zn−Cl(1)] has a significantly longer bond length than the equatorial chloride, and the amine in the other axial position [Zn−N(2), 2.411(2) Å] also has a longer bond length than the other coordinated nitrogens (average Zn−N(3,4) distance, 2.067 Å).

Figure 2 shows the crystal structure of complex **2**, which packs in the relatively uncommon space group $P6_5$. The asymmetric unit is composed of a single nickel complex. The Ni(II) coordinates to the ligand (L-MABO) through the oxime nitrogens, the amine nitrogen, and the thioether sulfur. Both chloride anions are also coordinated to complete a distorted octahedral coordination geometry. Selected bond distances and angles are given in Table 2. The chloride trans to the amine nitrogen of the complex, Cl(2), has a significantly longer bond length than Cl(1). The Ni−Cl(2) bond is also longer than the Ni−S bond. The amide arm participates in one classical intermolecular H-bond, (N(4)−H(4)···O(3); N(4)···O(3), 2.824(4) Å; H(4)···O(3), 1.95 Å).

The asymmetric unit of **3** is composed of two nickel complexes **a** and **b** (Figure 3a,b) with different coordination environments and a disordered $^1/_2$ methanol of solvation. Unlike the chloride complexes above, only one of the nitrate anions is directly coordinated to the nickel ion. It binds opposite the amine nitrogen in each molecule, while the second nitrate remains uncoordinated in the lattice. This additional available coordination site of the complex allows coordination of two of the available non-nitrogen, nonanion ligands (thioether, amide

Table 3. Selected Bond Distances (Å) and Angles (deg) of $NiC_{12}H_{24}N_5O_6S]NO_3 \cdot [NiC_{13}H_{28}N_5O_7S]NO_3$ (**3**)

3a		**3b**	
Ni(1)−N(1)	2.080(4) amine	Ni(2)−N(6)	2.115(4) amine
Ni(1)−N(2)	2.054(4)	Ni(2)−N(7)	2.049(4)
Ni(1)−N(3)	2.011(4)	Ni(2)−N(8)	2.028(5)
Ni(1)−S(1)	2.464(1)	Ni(2)−O(13)	2.113(4) methanol
Ni(1)−O(3)	2.078(3) amide	Ni(2)−O(9)	2.049(4) amide
Ni(1)−O(4)	2.024(3) nitrate	Ni(2)−O(10)	2.019(4) nitrate
N(1)−Ni(1)−N(2)	81.9(2)	N(6)−Ni(2)−N(7)	80.8(2)
N(2)−Ni(1)−N(3)	93.6(2)	N(7)−Ni(2)−N(8)	89.5(2)
N(3)−Ni(1)−N(1)	81.1(2)	N(8)−Ni(2)−N(6)	82.0(2)
N(1)−Ni(1)−O(3)	79.9(2)	N(6)−Ni(2)−O(9)	80.3(2)
N(2)−Ni(1)−O(3)	90.0(2)	N(7)−Ni(2)−O(9)	94.0(2)
N(3)−Ni(1)−O(3)	159.9(1)	N(8)−Ni(2)−O(9)	161.1(2)
N(1)−Ni(1)−O(4)	166.0(2)	N(6)−Ni(2)−O(10)	167.3(2)
N(2)−Ni(1)−O(4)	86.4(2)	N(7)−Ni(2)−O(10)	92.7(2)
N(3)−Ni(1)−O(4)	107.4(2)	N(8)−Ni(2)−O(10)	109.0(2)
N(1)−Ni(1)−S(1)	99.16(12)	N(6)−Ni(2)−O(13)	94.2(2)
N(2)−Ni(1)−S(1)	176.31(13)	N(7)−Ni(2)−O(13)	175.0(2)
N(3)−Ni(1)−S(1)	90.07(12)	N(8)−Ni(2)−O(13)	89.3(2)
O(3)−Ni(1)−S(1)	86.72(10)	O(9)−Ni(2)−O(13)	85.5(2)
O(4)−Ni(1)−S(1)	92.04(10)	O(10)−Ni(2)−O(13)	92.3(2)

oxygen, and/or solvent). In both **3a** and **3b** the amide is bound to nickel through the carbonyl oxygen. The thioether S(1) is only bound to nickel in complex **3a**, while the nickel in **3b** coordinates a methanol molecule O(13) in place of the thioether. Selected bond angles and distances are given in Table 3. Weak, nonclassical H-bonding occurs between the methyl group of the unbound thioether arm in **3b** and the coordinated NO_3^- of **3a** in addition to one of the NO_3^- counterions (C(24A)−H(24A)···O(19); C(24)···O(19), 3.507(8) Å; H(24A)···O19, 2.78 Å and C(24)−H(24A)···N(3); C(24)···N(3), 3.403(7) Å, H(24A)···N(3), 2.79 Å).

Spectroscopic Characterization. Absorption and CD spectra of 10 mM solutions of the Ni(II) complexes taken at approximately 1 h and 24 h after sample preparation were essentially identical. The aqueous and acetonitrile spectra with their Gaussian fits are shown in Figures 4 and 5, and the fit parameters are tabulated in Tables 4 and 5, respectively. The absorption and CD spectra of the zinc complex **1** in both acetonitrile and water are featureless below 33 000 cm^{-1}, as expected for a d^{10} metal. The absorption spectra of **2** and **3** in both water and acetonitrile show three bands typical of six-coordinate d^8 nickel complexes.[21] The absorption and CD spectra of **2** in acetonitrile, however, are markedly different from the others. The aqua color of this solution also differs from the deep blue-purple color of the others.

Coulometric measurements were obtained from aqueous and acetonitrile solutions of **2** and **3** for correlation with the interpretation of the solution spectroscopic data described in the Discussion section. In aqueous solution at the same concentration as the spectroscopic studies described above (10 mM), the conductivity of the chloride, **2** (82.7 S cm^2 mol^{-1}), is slightly higher than that of the nitrate, **3** (70.0 S cm^2 mol^{-1}). This difference is likely due to the difference in the nature of the anion rather than a difference in the number of ions in solution, as the conductivity of NaCl is slightly higher than the conductivity of $NaNO_3$ in water as well. In acetonitrile, however, the values are more than 20-fold higher for **3** (29.1 S cm^2 mol^{-1}) than for **2** (1.32 S cm^2 mol^{-1}). This is consistent with both chlorides of **2** remaining coordinated in acetonitrile to give a neutral complex while one or both of the nitrates is dissociated, as seen in the crystal structures. Similarly to the spectroscopic

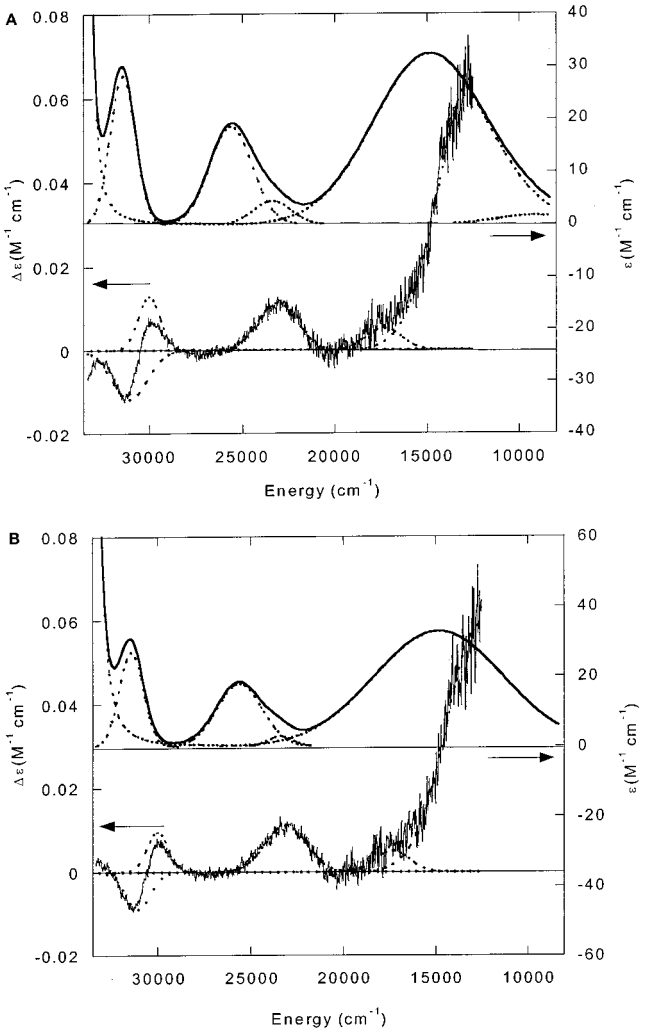

Figure 4. Absorption and CD spectroscopy (solid line) with fits (dotted lines) for (A) **2** in H_2O and (B) **3** in H_2O.

measurements, no differences were observed in the coulometric data collected 1 h after solution preparation compared to data collected after 24 h.

IR and Raman vibrational data were collected and are presented in Table S1 of the Supporting Information. The mid-IR spectra are reminiscent of the free ligand, while bands between 1500 and 1250 cm^{-1} indicative of nitrate in its different environments in complex **3** are not well resolved. In the far-IR, several bands in the energy range characteristic of ν(Ni−S) and ν(Ni−Cl) are observed for each complex between 300 and 100 cm^{-1}. The position and order of ν(Ni−S) and ν(Ni−Cl) bands has been shown to be dependent on the nature of the other ligands in the coordination sphere of previously described complexes.[22] Thus, definitive assignment of these bands is not possible without isotopic substitution studies.

Discussion

In the complexes reported here, L-MABO acts as a tridentate N_3 (**1**), tetradentate N_3S or N_3O (**2** and **3b**, respectively), or pentadentate N_3OS ligand (**3a**) demonstrating the wide range of possible conformations that can be achieved by this ligand. In all four molecules, the three nitrogen donors from the amine and two oxime groups make up one face of a pseudo-octahedron

(21) Lever, A. B. P. *Inorganic Electronic Spectroscopy*; Elsevier: Amsterdam, 1984.

(22) Schlapfer, C. W.; Saito, Y.; Nakamoto, K. *Inorg. Chim. Acta* **1972**, *6*, 284−290.

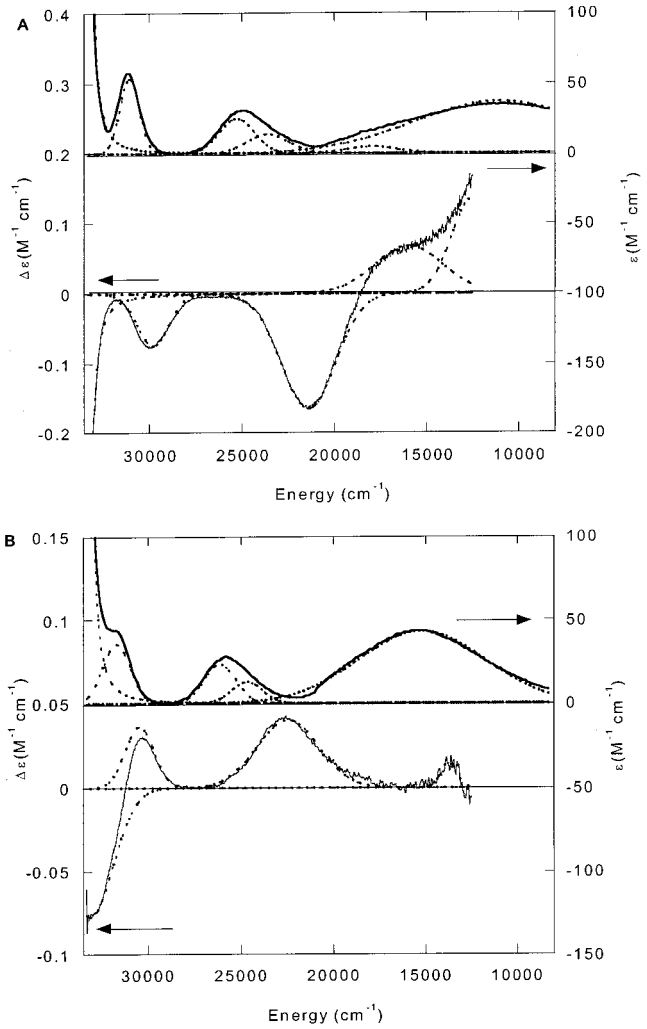

Figure 5. Absorption and CD spectroscopy (solid line) with fits (dotted lines) for (A) **2** in CH_3CN and (B) **3** in CH_3CN.

Table 4. UV−Vis (λ_{max}/cm^{-1} (ϵ/M^{-1} cm^{-1})) and CD ($\lambda_{(max\ or\ min)}$/cm^{-1} ($\Delta\epsilon$/M^{-1} cm^{-1})) in Water for Complexes **2** and **3**

2		**3**	
absorption	CD spectra	absorption	CD spectra
31420 (28.4)	31060 (−0.012)	31420 (26.9)	31060 (−0.009)
	30010 (0.013)		30010 (0.010)
25610 (18.6)		25610 (17.8)	
23400 (4.5)	23110 (0.011)	23400 (2.9)	23110 (0.011)
	17350 (0.005)		17350 (0.005)
14830 (32.5)		14830 (32.7)	
	<13000 (0.064)		<13000 (0.059)

Table 5. UV−Vis (λ_{max}/cm^{-1} (ϵ/M^{-1} cm^{-1})) and CD ($\lambda_{(max\ or\ min)}$/cm^{-1} ($\Delta\epsilon$/M^{-1} cm^{-1})) in Acetonitrile for Complexes **2** and **3**

2		**3**	
absorption	CD spectra	absorption	CD spectra
31030 (53.5)	29790 (−0.075)	31700 (35.4)	30480 (0.037)
25260 (24.9)		26140 (23.2)	
23600 (13.6)		24670 (12.8)	
	21420 (−0.165)		22480 (0.040)
17960 (4.6)			
	15950 (0.067)	15210 (43.0)	13740 (0.015)
11010 (36.9)			

(or trigonal bipyramid in the Zn complex). The other face in the nickel complexes consists of three weaker donors in terms of the spectrochemical series (thioether, amide carbonyl, nitrate, methanol, or chloride).

In zinc complex **1**, L-MABO acts as a tridentate N_3 ligand with two additional chlorides bound. Only the oxime nitrogens and amine of L-MABO coordinate to the metal center while the thioether and amide extend into the lattice. Although the already five coordinate zinc does not require an additional ligand, Ni(II) prefers a six coordinate geometry.[23] In **2**, L-MABO serves as a tetradentate N_3S ligand in which the nickel coordinates the thioether sulfur in addition to the amine and oxime nitrogens of L-MABO and the two chlorides. The uncoordinated amide arm extends into the lattice where it participates in H-bonding with two neighboring amides from other molecules. It is this H-bonding interaction that stabilizes the packing about a 6-fold axis, giving rise to an unbroken helical chain of amide H-bonds in the lattice. In nickel complex **3b**, L-MABO is bound through the carbonyl of the amide arm in addition to the oxime and amine nitrogens thereby acting as a tetradentate N_3O ligand. A methanol molecule and nitrate fill the fifth and sixth coordination sites, resulting in a +1 charge for the complex. The nickel in complex **3a** binds the thioether sulfur *and* the amide arm through its carbonyl oxygen in addition to the amine and oxime nitrogens of L-MABO, which thus serves as a pentadentate N_3OS ligand. In all of these nickel complexes, the bond lengths between the oxime nitrogen and the nickel are slightly shorter than those reported by Korvenranta et al.[24] for Ni(II) (average Ni−N, 2.119(18) Å). This may be due in part to the independence of each oxime arm in L-MABO as compared to the attachment of the oximes to imine bonds in the Korvenranta structure. Almost all the bond angles (L−Ni−L′) for the nickel complexes deviate from 90°, distorting the coordination sphere away from octahedral. This distortion is enforced by the steric constraints of the ligand. This can be clearly seen for the oxime arms that form five-membered rings with the nickel, giving more acute angles for N(oxime)−Ni−N(amine) (~80°) than for the angle between the two oxime arms (N(oxime)−Ni−N(oxime)), which approaches 90°. This angular distortion is also observed in the simpler [Ni(Tren)(H_2O)Cl]-Cl·H_2O complex.[25]

The denticity of the L-MABO ligand defines steric constraints that strongly influence the metal−amine bond lengths. In complex **2**, L-MABO serves as a tetradentate ligand, increasing the geometric constraint of the ligand relative to the tridentate case in **1**, resulting in a shorter M−N(amine) bond distance for **2**. In complex **3b**, L-MABO also serves as a tetradentate ligand, and its M−N(amine) bond distance is even shorter than that observed in complex **2**. The Ni−N(amine) bond length for complex **3b** is much more similar to that observed for [Ni(Tren)-(H_2O)Cl]Cl·H_2O [25] (Ni−N(tertiary amine), 2.105(3) Å) than for **2**. This likely results from the greater electrostatic attraction of nickel for the electron rich ligands in the charged complexes, as compared to the neutral complex **2**. In complex **3a**, L-MABO serves as a pentadentate ligand coordinating all available arms. This strictly constrains the geometry around the amine and, together with the positive overall charge, gives the shortest M−N(amine) bond of all of these complexes.

In contrast to the Ni−amine interactions, the Ni−thioether interaction is not significantly defined by the steric constraints of surrounding ligands. This makes complexes **2** and **3a** unusual compared to other Ni(II) complexes of mixed N/S ligands. Most such complexes have thioethers that are incorporated either into

(23) Cha, M.; Gatlin, C. L.; Critchlow, S. C.; Kovacs, J. A. *Inorg. Chem.* **1993**, *32*, 5868−5877.
(24) Korvenranta, J.; Saarinen, H.; Nasakkala, M. *Inorg. Chem.* **1982**, *21*, 1, 4296−4300.
(25) Marzotto, A.; Clemente, D. A.; Valle, G. *Acta Crystallogr.* **1993**, *C49*, 1252−1255.

a macrocycle or in the interior of a "linear" polydentate ligand. In these cases, other donor groups attached to both sides of the thioether moiety are coordinated to the nickel, restricting the available Ni−S bond length. In the "branched" motif of MABO, the methylthioether is free of these constraints and the Ni−S distance is determined mainly by the Ni−S electronic interaction. A search of the Cambridge Crystallographic Database shows only one other Ni(II) complex with at least three nitrogen ligands and a coordinated thioether free of the constraints of incorporation into a macrocycle or "linear" polydentate ligand.[26] That complex has a pendant methylthioether off of a N_4-macrocycle in an unusual 5-coordinate Ni(II) complex. Thus, these complexes with "branched" thioether coordination in a predominantly nitrogen coordination environment contribute a missing structure type to the pool of Ni(II) complexes with mixed N/S ligand sets.

The Ni−S bond length is longer in **3a** than in **2**, suggesting a weaker Ni−S interaction in **3a**. This may be due to that complex's overall charge of +1, which increases the nickel's preference for harder N/O ligands over the softer sulfur ligand, as compared to the neutral complex **2**. The relative "softness" of the nickel in complexes **3a** and **3b** appears to be modified by thioether coordination, with the nickel in **3a** (thioether bound) being softer than in **3b** (methanol bound). This difference in "softness" affects the bond lengths of the coordinated ligand groups. For complex **3a**, the difference between the Ni−O(amide) bond length and the Ni−N(oxime) bond length trans to Ni−O(amide) is 0.067 Å. This same difference for complex **3b** is 0.021 Å as the harder (relative to nitrogen) oxygen ligand [Ni(2)−O(9)] is more tightly bound in **3b** than in **3a**. As noted above, the Ni−N(amine) bond distances are strongly affected by the steric influence of the ligand framework, and therefore comparison to the Ni−O(nitrate) ligands trans to them does not show the influence of the relative "softness" of the nickel on these bond distances. This effect of thioether coordination on the relative Ni−O and Ni−N bond lengths in these complexes nicely demonstrates how metalloenzymes may use coordination of amino acid side chains that are not directly involved in catalysis to change the relative activation of the other metal−ligand bonds that are important to the catalytic mechanism.

To analyze differences between the crystallographically determined structures of the Ni(II) complexes and their structures in solution, the absorption and CD spectra of **2** and **3** in both water and acetonitrile solutions were obtained. The absorption spectrum in the ligand field region (300−1200 nm) of each solution shows the three bands generally observed in six-coordinate octahedral or pseudo-octahedral Ni(II) complexes, corresponding to the spin-allowed transitions from the $^3A_{2g}(F)$ ground state to the $^3T_{2g}(F)$, $^3T_{1g}(F)$, and $^3T_{1g}(P)$ excited states of the d^8 ion in O_h symmetry.[21] However, the distortion of these complexes away from true O_h symmetry affects their spectroscopic features. The intensity of the bands is increased compared to more rigorously octahedral complexes, suggesting a reduction in the Laporté forbidden nature of the transitions in O_h symmetry. Additionally, the "degenerate" transitions show energy splittings, observed in both the Gaussian analysis of the absorption bands and the positions of the circular dichroism bands that appear due to the chirality of the complexes which have true C_1 symmetry. The affect of the deviations from O_h symmetry on the spectroscopy may be understood by considering the distortions in terms of successively descending symmetries from the highly idealized O_h to the true C_1 point group.

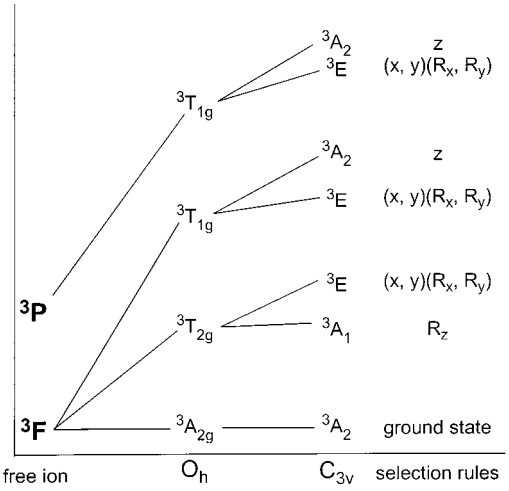

Figure 6. Qualitative correlation diagram for the triplet states of the d^8 ion in O_h and C_{3v} symmetry. The selection rules for the transitions to each excited state in C_{3v} are listed to the right in terms of electric (x, y, z) or magnetic (R_x, R_y, R_z) dipole character.

As the aqueous solutions of the two Ni(L-MABO) salts demonstrate essentially identical absorption and CD spectra, it is reasonable to assume that all anions and the amide and/or thioether groups coordinated in the solid state are displaced by water molecules. We shall first consider the spectra of these aqueous solutions and then compare differences in the acetonitrile solutions. In the solid state nickel complexes, the three nitrogen donors from the amine and two oxime groups make up one face of the pseudo-octahedron, while three weaker donors in terms of the spectrochemical series make up the opposite face (presumably all displaced by waters in the aqueous solutions). This arrangement suggests a small C_{3v} distortion from O_h symmetry, with the C_3 axis going through the centers of the N_3 and O_3 faces. This C_{3v} distortion should split the excited states as shown in the qualitative correlation diagram for the triplet states of the d^8 ion in Figure 6. The electric (x, y, or z) or magnetic (R_x, R_y, or R_z) dipole allowed character of the transition to each state in C_{3v} symmetry is listed to the right. Electric dipole allowed transitions are expected to have some absorption intensity, while CD intensity requires that the transition is both electric and magnetic dipole allowed *along the same axis*. This does not occur for any nondegenerate representation in the nonchiral C_{3v} point group, nor do the electric and magnetic dipoles transform along the same axis in the individual components of the degenerate E representation. However, the true C_1 symmetry mixes, for example, some z character into the transition that transforms as R_z, allowing the transition to be CD active. As a result, transitions that are magnetic dipole allowed are expected to have the greatest CD intensity relative to the absorption intensity.[27]

In the Gaussian deconvolution of the aqueous solution spectra, we see an intense, positive CD feature with a maximum below 13 000 cm^{-1}, another positive but weaker CD band at 17 350 cm^{-1} that appears as a shoulder on the first band, and a broad absorption band centered at 14 830 cm^{-1}. These correspond to components of the lowest energy transition to the $^3T_{2g}$ state in O_h symmetry. The energy of the $^3T_{2g} \leftarrow {}^3A_{2g}$ transition in octahedral complexes corresponds to 10 Dq. Using the absorption maximum, this gives a Dq value of 1483 cm^{-1}, which is unusually high for Ni(II). However, trigonal distortions to O_h

(26) Schmid, C. L.; Neuburger, M.; Zehnder, M.; Kadan, T. A. *Helv. Chim. Acta* **1997**, *80*, 241−252.

(27) Gillard, R. D. In *Physical Methods in Advanced Inorganic Chemistry*; Hill, H. A. O., and Day, P., Eds.; Interscience Publishers: New York, 1968.

symmetry are known to give anomalously large values of Dq based on this absorption energy.[28] An absorption band at 25 610 cm^{-1} with a weak, lower energy band at 23 400 cm^{-1} that causes an observable asymmetry to the band shape and a positive CD band at 23 110 cm^{-1} make up the lower symmetry components of the $^3T_{1g}(F) \leftarrow {}^3A_{2g}$ transition. An absorption band at 31 420 cm^{-1} and a pair of CD bands at 30,010 cm^{-1} (positive) and 31 060 cm^{-1} (negative) make up the $^3T_{1g}(P) \leftarrow {}^3A_{2g}$ manifold. Based on the C_{3v} selection rules indicated in Figure 6, the lowest energy set of transitions should include one component that is dominated by its CD intensity, corresponding to the transition to the $^3A_1$ state, and another E pair that is further split by the lower, true symmetry of the complex. If this lower symmetry distortion is predominantly C_s in nature, due to a mirror plane through the one amine donor that bisects the two oxime donors, then the two "E" components will correspond to A′ and A″ symmetry in C_s, each of which is both electric and magnetic dipole allowed, but not along the same axis. Thus, uneven distribution of CD and absorption intensity is expected. The intense lowest energy CD band is assigned as the magnetic dipole allowed transition to $^3A_1$ in C_{3v}, while the absorption and CD maxima at 14 830 and 17 350 cm^{-1} are assigned as the components of the ^3E transition. Likewise, the more intense component of the $^3T_{1g}(F)$ manifold at 25 610 cm^{-1} is assigned as the electric dipole allowed transition to $^3A_2$, and the weaker absorption band and the CD band at 23 340 and 23 110 cm^{-1}, respectively, correspond to the split E pair. Finally, the absorption band at 31 420 cm^{-1} could be assigned to the electric dipole allowed transition to $^3A_2$ in the P manifold. However, the energy difference between the A_2 and E components of the P manifold of trigonally distorted Ni(II) complexes has been calculated to be much smaller than the differences in the F components.[28] Thus, the A″ component of the C_s−split E pair should mix strongly with the transition to A_2 (which correlates to A″ in C_s), so the absorption and CD intensity of the three observed bands tightly clustered between 30 000 and 31 500 cm^{-1} should not be specifically assigned to the different components of the ^3P transition manifold in C_{3v} symmetry.

The spectra of **3** in acetonitrile solution are very similar to the aqueous spectra, except for small shifts in the band positions, and some redistribution of absorption and CD intensity. It is likely that solvent molecules, or perhaps trace water in the solvent, displace the non-nitrogen donor groups as in the aqueous solution, although maintaining coordination of one nitrate in acetonitrile is not ruled out. The spectra of **2** in acetonitrile, on the other hand, are quite different. Most notably, the broad, low-energy absorption band is 4000 cm^{-1} lower in energy than the corresponding band in the other absorption spectra. This is consistent with the chloride anions remaining bound in the acetonitrile solution, as Cl^- is lower in the spectrochemical series than water, resulting in the lower observed Dq value. Also, the CD feature at 21 420 cm^{-1} is more intense and opposite in sign compared to the corresponding features in the other CD spectra. The presence of one or two chloride ligands changes the relative contributions of the C_{3v} and C_s distortions from O_h, resulting in the observed differences in the relative intensities of the absorption and CD bands compared to the other three solutions.

Occasionally, spin−orbit coupling of the spin-allowed transitions to spin-forbidden transitions in the ^1D manifold (not shown in Figure 6) are observed for Ni(II) complexes.[21] The lowest energy singlet state is generally observed around 12 500 cm^{-1},[28] and may be responsible for the increased breadth and poorer fit of the lowest energy absorption band in the solution of **2** in acetonitrile relative to the other solutions. In any case, the similarity of the ligand field spectra of the aqueous solutions and the acetonitrile solution of the nitrate salt, compared to the acetonitrile solution of the chloride salt, strongly supports the displacement of all of the non-nitrogen ligands by solvent molecules in solution, except in the case of **2**, which retains its chloride ligands in acetonitrile solution. This is consistent with our conductivity measurements that indicate the same number of ions in the aqueous solutions of both **2** and **3**, and at least one uncoordinated nitrate in the acetonitrile solution of **3**, while the acetonitrile solution of **2** contains mainly a neutral complex. The literature also shows that thioether coordination to Ni(II) in solution usually only occurs in very weakly coordinating solvents such as nitromethane,[29,30] although thioether coordination in acetonitrile[31] and other potentially coordinating solvents[26] has been reported.

The versatile pendant arms of L-MABO permit coordination as a tri-, tetra-, or pentadentate ligand. This rich variety of donor groups has been shown through the crystallographic data to provide the four different coordination sets N_3, N_3S, N_3O, and N_3OS in the solid state. The thioether-bound complexes represent unusual coordination environments for structurally characterized Ni(II) complexes in that they include a "branched" thioether ligand in a predominantly nitrogen coordination environment. This results in a Ni−S distance that represents the "inherent" bond strength rather than the steric constraints of the surrounding ligands, which may be useful for comparison to biological nickel sites. The geometric constraints of the ligand do impact the metal−amine nitrogen bond length, however, with greater denticity resulting in shorter bond lengths. The overall charge (based on coordinated anions) and relative hardness (mediated by thioether coordination) of the metal center change the relative bond lengths of the remaining pendant arms of L-MABO. The absorption and CD solution spectra, as well as conductivity measurements, suggest that the weak donors are displaced by water in aqueous solution. In acetonitrile, however, complex **2** retains the chloride ligands in its coordination sphere. The spectroscopic studies of these complexes demonstrate the utility of a "descent in symmetry" model for the analysis of ligand field spectra when sufficient data, especially from circular dichroism, are available.

Acknowledgment. The authors wish to thank Prof. Apryll Stalcup (University of Cincinnati) for use of her CD spectropolarimeter. Funding was provided by the Petroleum Research Fund administered by the American Chemical Society (ACS-PRF 33960-G3) and the Department of Chemistry, University of Cincinnati.

Supporting Information Available: Crystallographic data in CIF format and a table of Raman and IR data for solids **1**, **2**, and **3**. This material is available free of charge via the Internet at http://pubs.acs.org.

IC000971F

(28) Alper, J. S.; Zompa, L. J. *J. Inorg. Nucl. Chem.* **1980**, *42*, 1693−1696.
(29) Smith, G. F.; Margerum, D. W. *J. Chem. Soc., Chem. Commun.* **1975**, 807−808.
(30) Desper, J. M.; Gellman, S. H.; Wolf, R. E.; Cooper, S. R. *J. Am. Chem. Soc.* **1991**, *113*, 8663−8671.
(31) Kulatilleke, C. P.; Goldie, S. N.; Ochrymowycz, L. A.; Rorabacher, D. B. *Inorg. Chem.* **1999**, *38*, 5906−5909.